

# Numerical simulation of a conical roofed low-rise building to estimate the wind pressure coefficients

Jagbir Singh\* & Amrit Kumar Roy

Civil Engineering Department, National Institute of Technology Hamirpur, HP, 177005, India

\*Corresponding Author: [jagbir@nith.ac.in](mailto:jagbir@nith.ac.in)

**ABSTRACT:** The roof shape and the slope of the roof are both significant constraints for the protection of the structure against wind load. The present study aims to investigate the variation of wind pressure coefficients on the conical roof and to observe the wind behavior around the building. CFD (Computational Fluid Dynamics) software ANSYS has been used for modeling and simulation. It is found that the 35° roof slope is the optimum roof angle for the present study, as there is the least area-weighted average pressure coefficient for this roof angle. While the roof slope 30° is found the most critical roof angle in terms of wind load resistance among all the roof angles of the present study.

**KEYWORDS:** Conical roof, Velocity profile, Horizontal Homogeneity, Roof angle, Wind Pressure coefficient, Velocity streamline.

## 1. INTRODUCTION

Wind load (in form of cyclones, hurricanes, storms, gales etc.) is an important type of loadings that each building face. Past reports show that the high winds cause a huge loss of lives and properties [1]. Also, the gust which is high speed wind for few seconds (during a storm or cyclone) have a very strong effect on buildings and other objects [2]. Strong winds affects the strength and serviceability of the buildings also [3]. The wind load affects all parts of a building, and when it comes to wind load, a roof is a much important part of a building, may it be high-rise or low-rise. There are a lot of roof shapes, and all shapes have their features [4]. As the roof of a house accounts for 3% of the total cost of house construction only, a roof is much more important than that. Apart from the selection of material, the design and construction give personality to the roof.

Some people may not be aware that they have multiple varieties concerning roof design, as in Figure 1, illustrating the 20 most common roof styles. All these roofs have their pros and cons, considering roof styles, design & architecture.

There are different methods to investigate the wind load and, the CFD modeling and simulation is one of them. CFD study or numerical study is useful to determine the velocity streamline, magnitude of pressure coefficients, velocity vectors, vortex shedding and several associated constraint variables, etc. through the model exterior [5]–[7]. However, a lot of research work is being carried out using CFD simulation as a replacement for the wind tunnel experimentation, and the outcomes attained are sufficiently reliable with the experimental outcomes [8]–[14].

Various wind codes like IS 875 (Part 3): Indian Standard Design Loads, Minimum Design Loads for Buildings and Other Structures, and Australian/New Zealand Standard (AS/NZS) - Structural Design Action, Part Wind Action are also used worldwide to investigate the wind loads [15]–[19]. And the wind load norms for a pyramidal roof building are usually not recorded in wind codes. Also, most of the research work in this area is related to low-rise structures (buildings with height less than 20m and 18.3m, as per Indian and American wind standards, respectively [18], [20]) having canopy roof, gable roof, hip roof, isolated pitched roof [21].

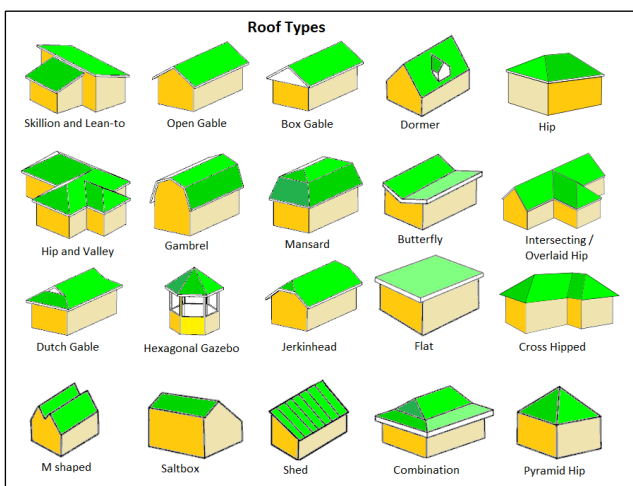


Figure 1: Top 20 of the most popular roof styles [4]

Also, a pyramidal roof has very different aerodynamic characteristics and a unique behavior to the wind flow and was found with the lowest uplift, on comparison with the gable roof and the hip roof [22]. However, inadequate research has been performed in this particular area (i.e., the influence of wind force on pyramidal roof-shaped structures) [23]. Hence, it is necessary to observe the wind flow and wind force on different types of pyramidal (with base square, rectangle, pentagonal, conical etc.) roofed structures.

So, in the current study, the influence of the roof slope on the scattering of the wind load on the roof surface of low-rise buildings having a conical roof is investigated through CFD simulation. As previously told that a hip roof was found better than a gable roof, and the pyramidal roof was found better than the hip roof from the viewpoint of wind load. Therefore, the conical roofed (which is also a form of pyramidal roof) low-rise building is taken for the present study.

After a brief introduction to the present study, there is a description of the CFD simulation process in section 2, where all steps of the CFD process are discussed briefly. The CFD Results have been discussed in section 3, and this section contains horizontal homogeneity of the velocity profile, pressure coefficients, and velocity streamlines. While section 4 explains the limitations of the

present study and, finally, in the last section of the study, i.e., the conclusion has been given.

## 2. CFD SIMULATION PROCESS

The investigation of the variation of wind pressure coefficients on the conical roof and the wind behavior around the building has been carried out in the present study. CFD modeling and simulation have been used for the analysis. There are mainly four steps in the CFD process, i.e., model creation, mesh generation, to set the boundary conditions, solver setting, simulation run, and extraction of results.

The geometry of the model can be import from other software or can be created in ICEM CFD. ANSYS tool ICEM CFD has been used to create the model and to generate the mesh. For the boundary condition and solver setting, and later to run the simulation, Ansys Fluent has been used. There are few more software to extract the results like Fluent, CFD-Post, Tecplot, etc., and in the present study, both fluent and CFD-Post have been used.

### 2.1. Model Creation

With different roof angles, i.e.,  $20^\circ$ ,  $25^\circ$ ,  $30^\circ$ ,  $35^\circ$ , and  $40^\circ$ , ICEM CFD is used to create five conical roof building models. The plan area of the building

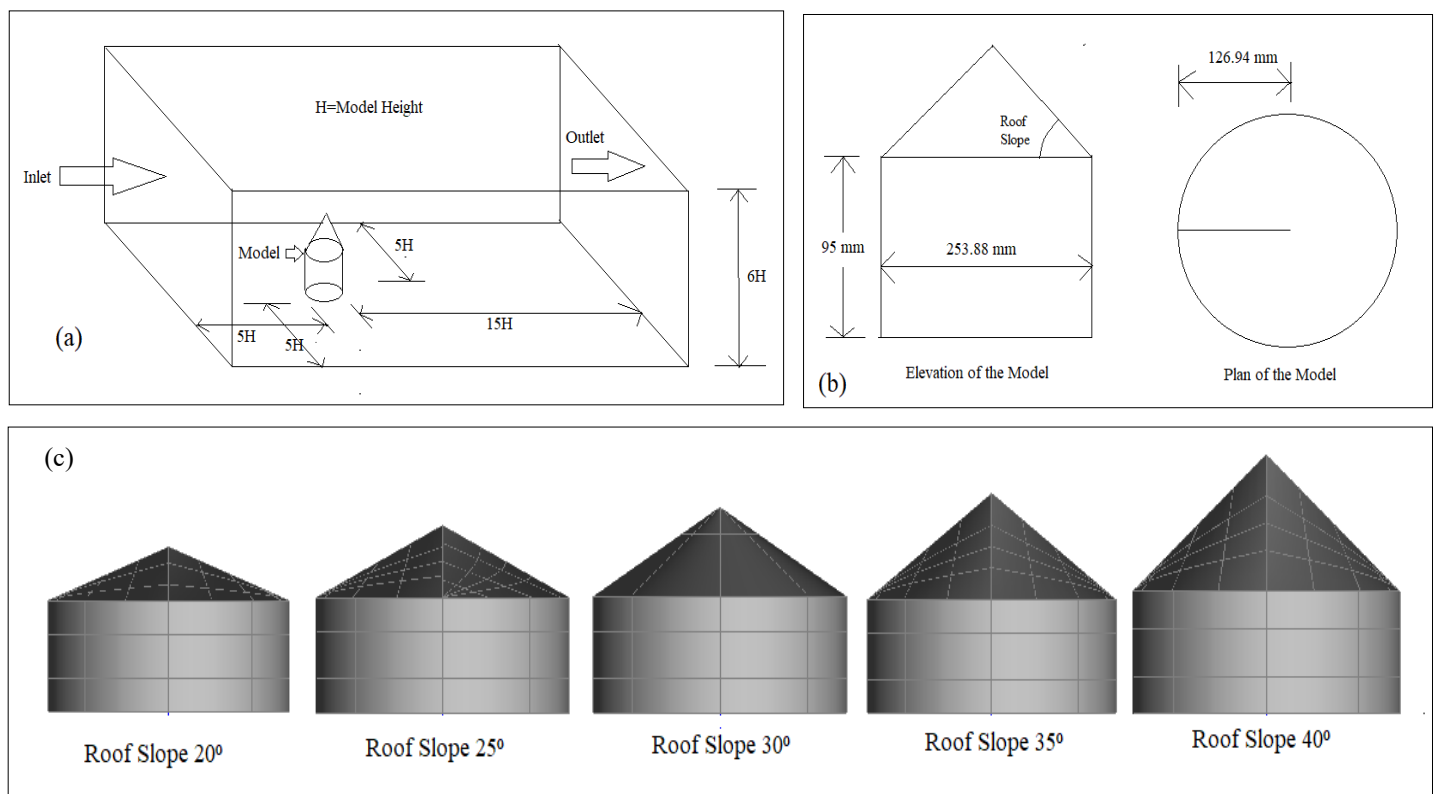
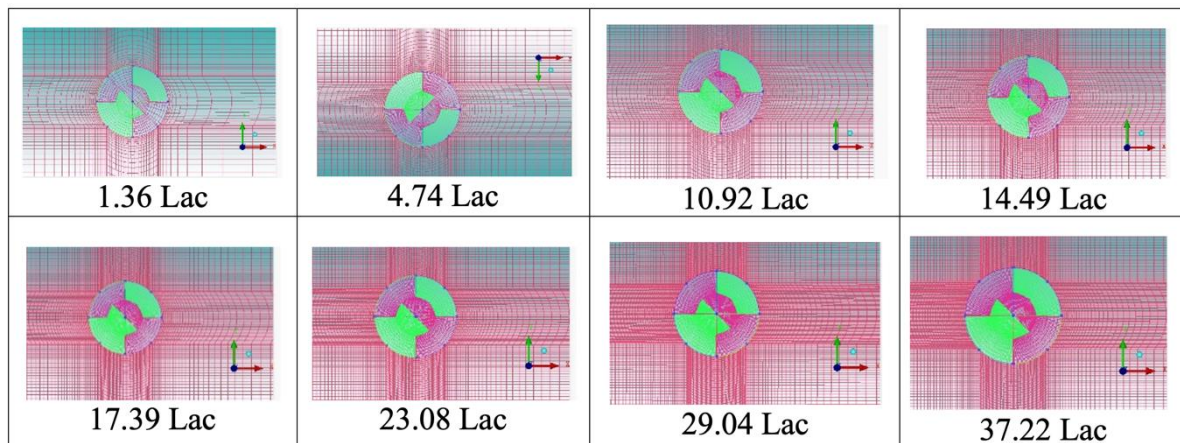


Figure 2: (a). Computational domain, (b). Geometry of Building Model and Figure 2(c). Different conical roof models with various roof slopes

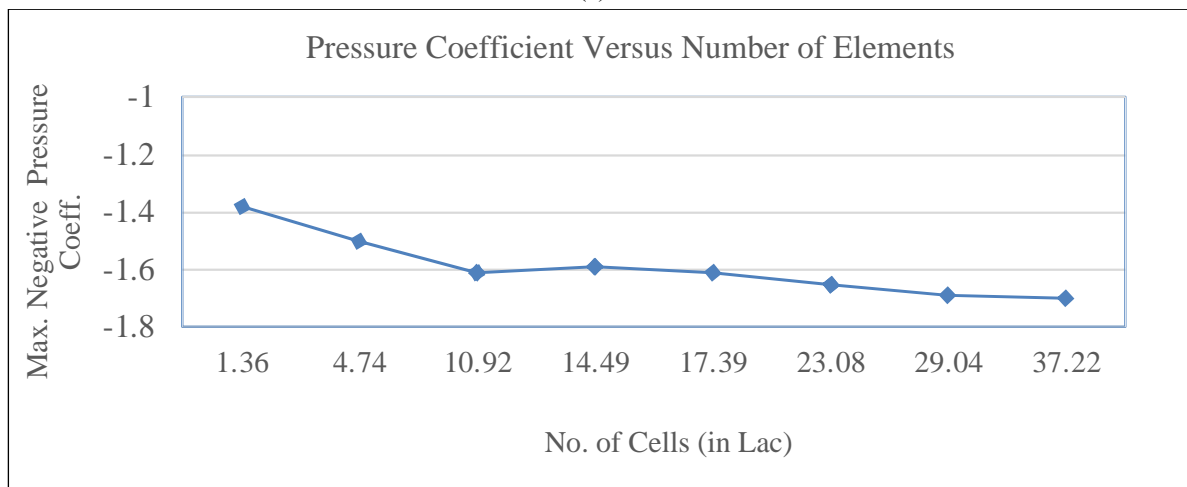
model and the height of the present building model is collected from a study conducted at CBRI in Roorkee (India), [24] and the dimensions of the domain for the current study are taken from the Revuz et al. study [25]. The domain specifications are shown in Figure 2(a). A scale of 1/25 has been taken for the measurements.

The domain specifications used in the present study are taken from Revuz’s study, as mentioned earlier. In Revuz’s study, the inlet is at a distance of  $5 \times H$  ( $H$  is the height of the model) from the front of the building model. And the outlet is  $15 \times H$  away

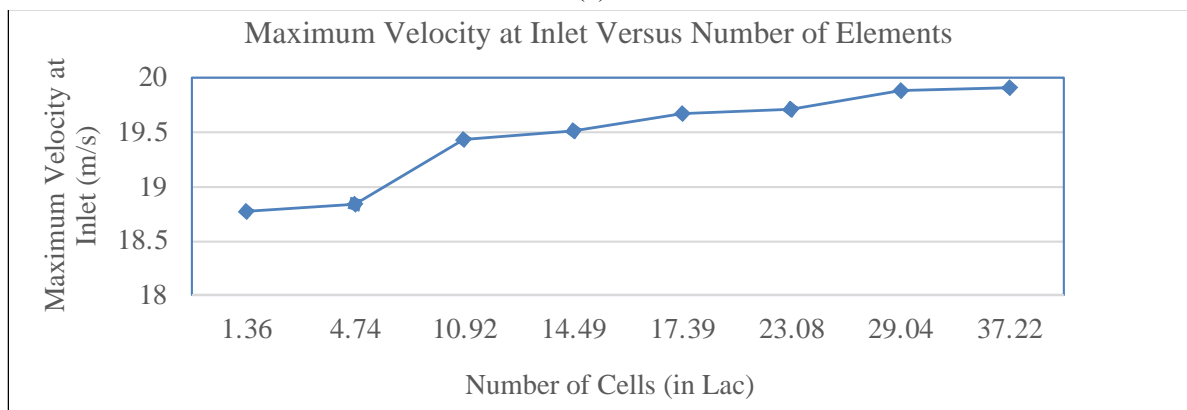
from the backside of the building model (in along wind direction). The sides of the domain are  $5 \times H$  away from the model, and there is a  $6 \times H$  height of the domain. In Figure 2(b), the building model with the measurements, the elevation, and the plan of the building model are shown, while different building models for various roof slopes are shown in Figure 2(c). The base radius of the building model is taken as 126.94 mm, and the eave height of the model is considered as 95 mm.



(a)



(b)



(c)

Figure 3: (a) Different meshings (by varying number of cells), (b) Pressure Coefficient Versus Number of Cells, (c) Maximum Velocity at Inlet Versus Number of Cells

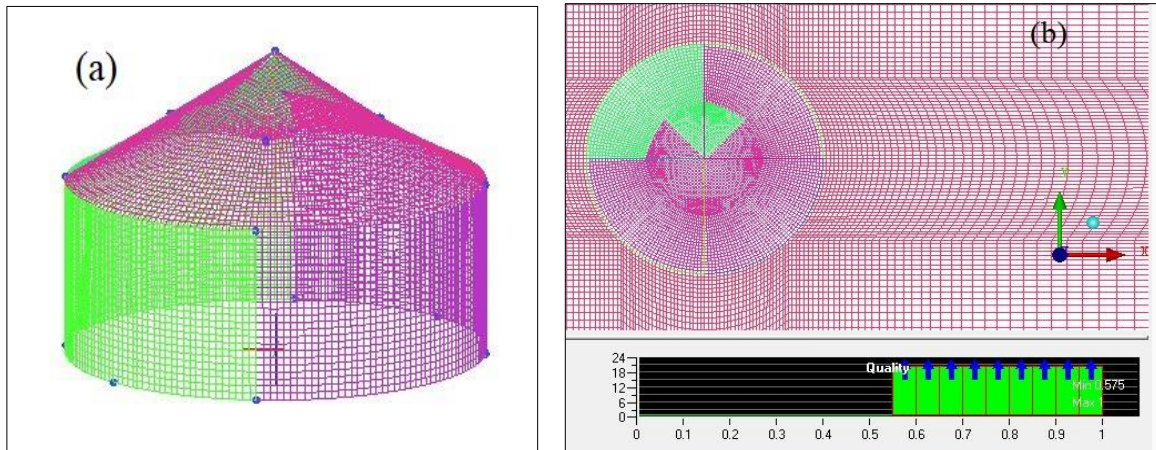


Figure 4: (a) Building model Meshing and, (b) CFD domain Meshing with mesh quality assessment

## 2.2 Mesh Generation

All the models are formed in ICEM CFD, as presented in Figure 2. The mesh quality governs the simulation time and the result precision, so an acceptable fine mesh is essential nearby the building model. The meshing is obtained by using a structural hexahedral grid. A reasonable fine mesh has been used for the building models and is displayed in Figure 4(a).

### 2.2.1 Mesh Sensitivity Analysis

The most basic and precise method for valuing mesh quality is to refine the mesh until a critical result. The mesh is refined up to a level, at which the results don't alter with further refinement. And in results, any parameter like pressure coefficient, wind velocity, force coefficient, etc., can be checked for different meshings.

The appropriate mesh is achieved by extracting the pressure coefficients and the inlet velocity for the building model with a 20° roof slope for different meshes (by varying the number of cells). In Figure 3(a,b,c), different grids, and respective outcomes have been illustrated. The various grids have been generated in ICEM CFD for 1.36, 4.74, 10.92, 14.49, 17.39, 23.08, 29.04, and 37.22 lac cells.

For a different cell number, the magnitude of pressure coefficient and inlet velocity has been improved with an increase in the number of cells. A sixteen lac increase in the number of cells (1.36 lac to 17.39 lac) gives rise to the pressure coefficient and the inlet velocity by 17% and 4.8%, respectively. For further increase in cells, i.e., 23.08, 29.04 and 37.22 lac, there is an increase of

20%, 22%, 22% in pressure coefficient while it is 5%, 6%, 6% for inlet velocity respectively. So, in the present study, a grid with 23.08 lac cells has been chosen as a grid with a very large number of cells (very fine mesh) require extra resources, and it increases the simulation time.

The models with reasonable mesh quality as illustrated in Figure 4(a,b), can be ensured by checking the quality of each model. In the current study, the mesh quality is more than 0.55 for all models, as presented in Figure 4(b). In ANSYS tools, ICEM CFD is used to assess the mesh quality, and if the quality of the mesh is more than 0.5 (on a scale of 0.0 to 1.0), then it is classified as good as per the Ansys tool guideline [26].

## 2.3 Boundary condition

Only the appropriate boundary conditions, essential to simulate the real flow, can display the actual physical fluid flow. For the inlet and outlet of the domain, it is necessary to define the specific boundary conditions for an accurate result, which may be difficult at all instances of time. At the windward boundary, the velocity inlet has been used with the subsequent expressions for the wind component of velocity.

Velocity,  $U$ , and turbulence intensity,  $I$ , which are fluctuated with the height of the inlet domain, is nearly the same to the wind tunnel study carried out by Roy, et al. 2012 and is presented in Figure 5, [27]. A standard illustration of the ABL (Atmospheric Boundary Layer) velocity profile is as displayed below in equation (1).

$$U(z) \frac{k}{u_*} = \ln \left( \frac{z + z_0}{z_0} \right) \quad (1)$$

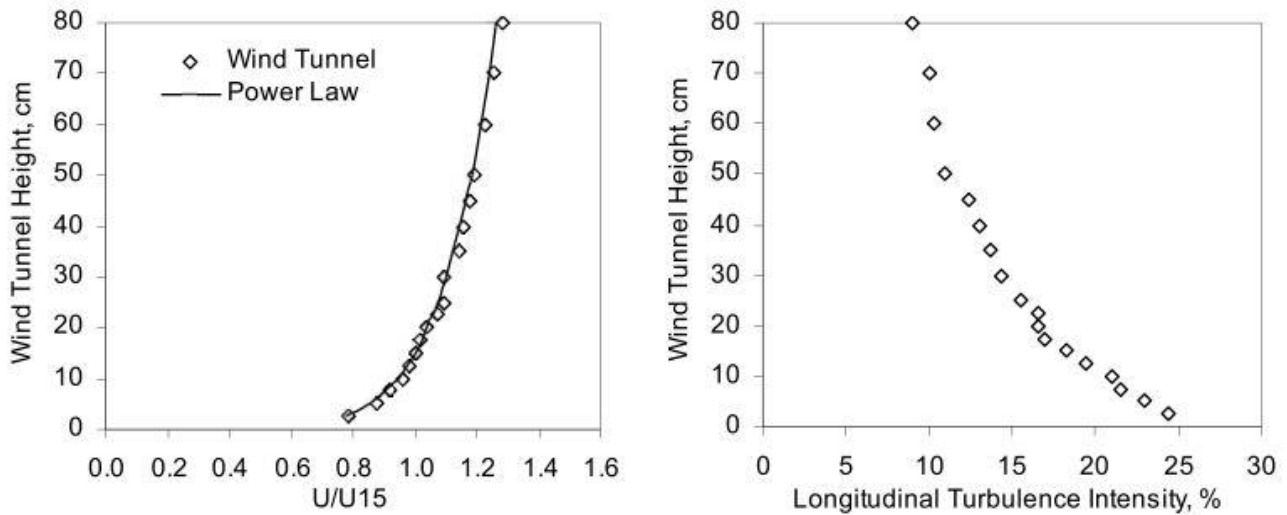


Figure 5: The wind velocity profile (U), and turbulence intensity (I), from a wind tunnel study, has been used for CFD simulation [27]

The sidewalls and the top of the domain are displayed as slip walls means normal velocity and normal gradients of all variables are nil. The static pressure at the outlet is specified as zero.

#### 2.4. Solver parameters

The finite-volume method has been used in ANSYS Fluent to solve the principal equations and related case-specific boundary conditions. The finite element method is the process of dividing the model into small units or minor isolated parts, which are identified as finite elements. The dimensions of the stiffness matrix are governed only by the number of nodes, and the outcomes are modified by expanding the collocation points and number of nodes [28]. Individually, in Fluent, a component has its governed equations & these components are stored as a global matrix.

As indicated earlier, the explanations are steady-state. For the turbulence, momentum and pressure equations, second-order differencing, and the “coupled” pressure-velocity coupling method are utilized. These are used because of their influence on steady-state in single-phase flow problems.

The usually applied benchmarks for residuals chop down is to fall to 0.0001 from their initial values after finishing a few hundred iterations. Also, the simulation is supposed to be converged when the drag, lift, side forces and the moments subjected to the building model are reached to the static values. There is some deviation of less than 1% in the “steady” values of the several monitoring values when the simulations are in steady-state.

### 3. RESULTS AND DISCUSSIONS

In the current study, different pyramidal roof building models have been simulated through the ANSYS Fluent. All the building models have the same plan shape, various roof slopes, and also various wind directions. To spot the variation in wind pressure distribution on the internal roof surface with changing roof slopes is the key objective of this study.

#### 3.1 The Horizontal Homogeneity among Different Velocity Profiles

The horizontal homogeneity is the comparison among different velocity profiles and the deviation of velocities at the upwind side of the building model in the computational domain. From line no. 1 to 6, a total of 6 nos. of vertical locations are created @ 200mm interval between two consecutive lines to spot the horizontal homogeneity among different velocity profiles as displayed in Figure 6(a). In Figure 6(b) for different vertical lines, i.e., lines 1 to 6, the respective velocity profiles have been shown. It is noticed that at building model height, the wind speed is near about 11m/s, validating the velocity profile.

It is additionally observed that line 6, which is located on the front wall of the building model, has zero velocity at some points (represented by pink color). These points are stagnation points. That is because of the wind striking on the front wall of the building model, and the deviation of velocity is highest for line 6 up to the model’s height, which is due to the cylindrical shape of the wall and conical roof shape.

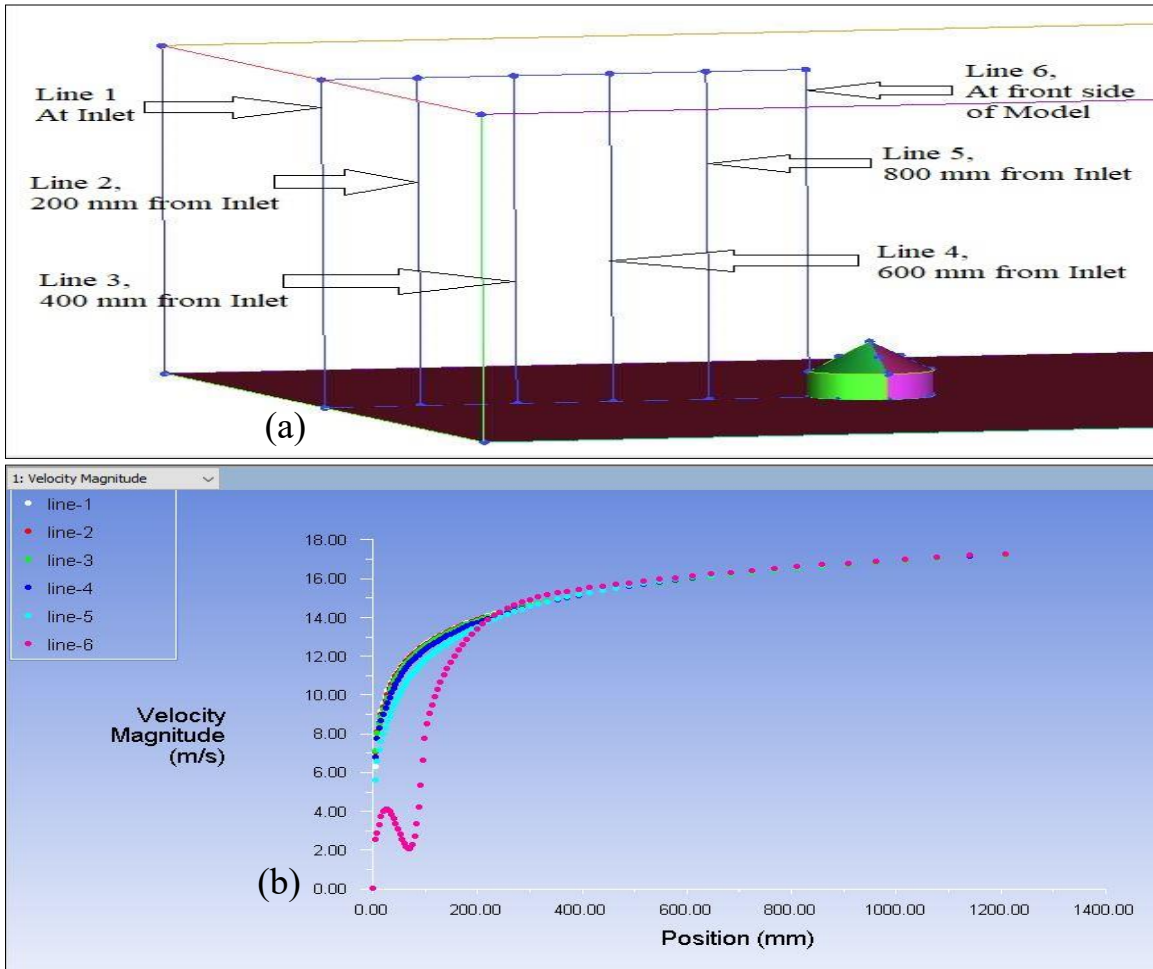


Figure 6: (a) Locations for plotting velocity profiles and (b) horizontal velocity profile homogeneity at the windward side

White, red, green, dark blue, aqua and pink colors of different velocity profiles represent lines 1, 2, 3, 4, 5, and 6, respectively. There are noticeable variations in velocities of all the velocity profiles up to some height, and it is because of the locations of different lines and disturbances caused by the building model. And at some specific height, velocity becomes constant. This velocity is known as gradient velocity, and the respective height is known as gradient height.

### 3.2 Wind Pressure Coefficients on the internal roof surface of the building

To further investigate the influence of the roof angle on the distribution of pressure coefficients on the external roof surface of the building, Figure 7(a) displays the outline of roof geometry and acting wind pressure. In contrast, Figure 7(b) represents the contours of the pressure coefficient ( $C_p$ ). The wind pressure coefficient is calculated as displayed in equation (2):

$$C_p = \frac{(P - P_s)}{0.5\rho U_{Ref}^2} \quad (2)$$

Where, static pressure is denoted by  $P$  and the reference static-pressure by  $P_s$  in equation (2),  $\rho$  is the air density =  $1.225 \text{ kg/m}^3$ , and in the approach flow,  $U_{ref}$  denotes wind velocity at the building height ( $U_{ref} = 9.81 \text{ m/s}$  at  $z = 0.11 \text{ m}$ ). By using ANSYS Fluent, contours of pressure coefficients for various roof angles, i.e.,  $20^\circ$  to  $40^\circ$  @  $5^\circ$  interval has been plotted and are displayed in Figure 7(b).

Different colors represent the contours of the pressure coefficient. The red color shows the maximum positive pressure region, i.e., positive pressure coefficient (0.010 to 0.24) and it varies with the change in roof slope. And the dark blue color indicates the maximum negative pressure (suction) region, i.e., area show the maximum negative pressure coefficient (-1.8 to -2.1) in the present study.

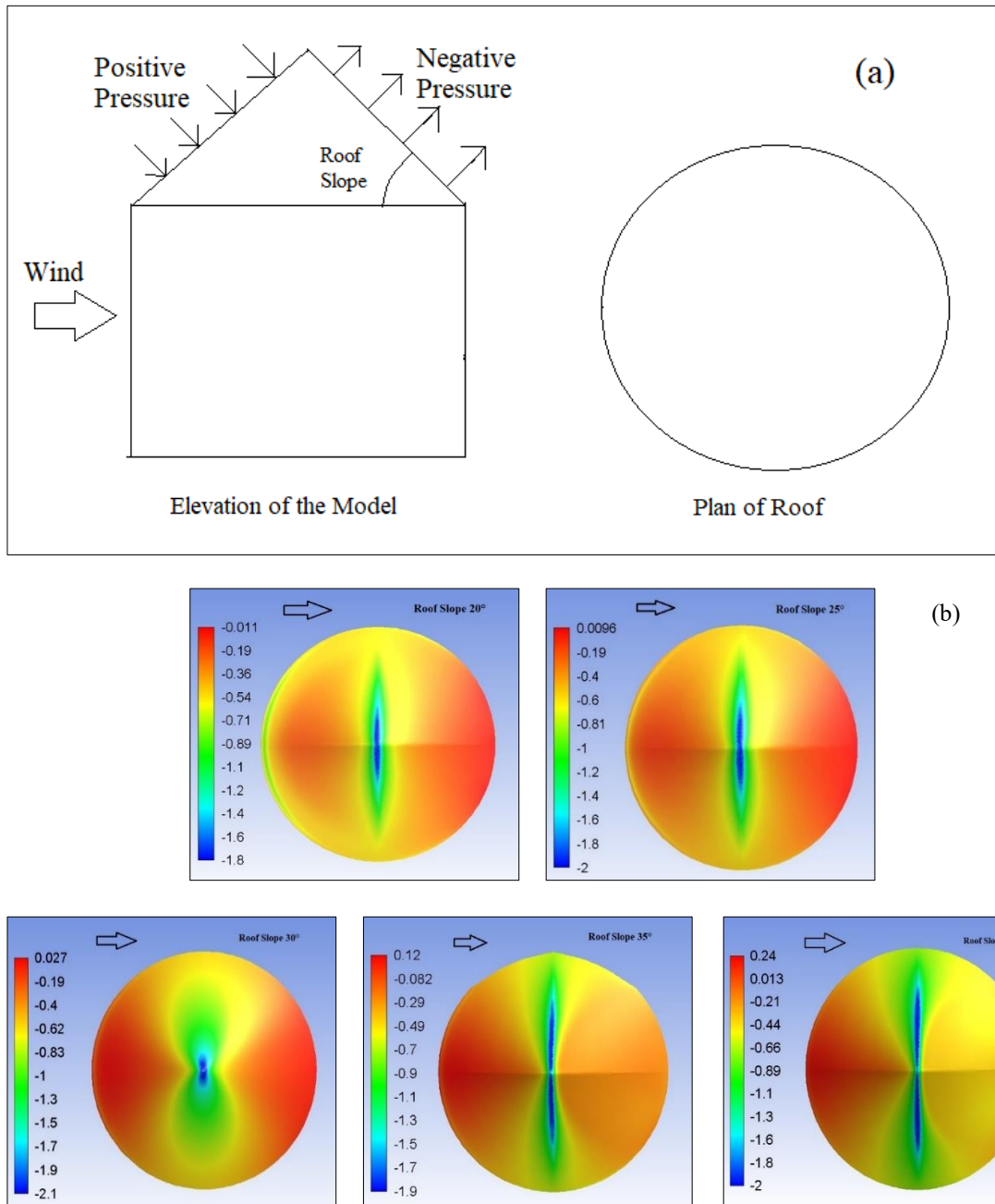


Figure 7: (a) Outline of roof geometry and acting wind pressure, (b) Contours of maximum pressure coefficients for different roof slopes @ 5° interval

In the case of a 20° roof slope, the whole roof surface has negative pressure due to a minimal roof angle. Among all the wind angles, the highest maximum positive wind pressure coefficient is found as 0.24 in case of a 40° roof angle. In contrast, the highest maximum negative pressure coefficient (suction) is seen as -2.1 in the case of a 30° roof slope.

It is observed from the pressure coefficient contours that the area of maximum negative pressure is least in case of a 30° roof slope, as the higher roof slopes cause more vortices and whirls around the model. Also, the variation of pressure coefficients shows a symmetrical pattern for all the roof slopes along the centerline (along wind

direction). The pattern of pressure coefficient variation is different for almost all roof slopes; in

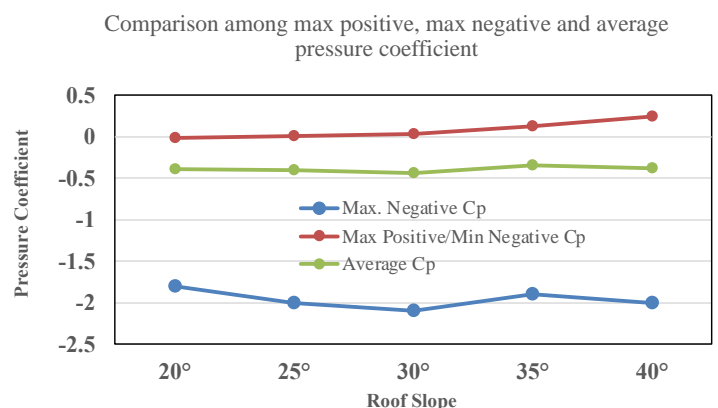


Figure 8: Variation of pressure coefficients (Cp) with the change in roof slope (α)

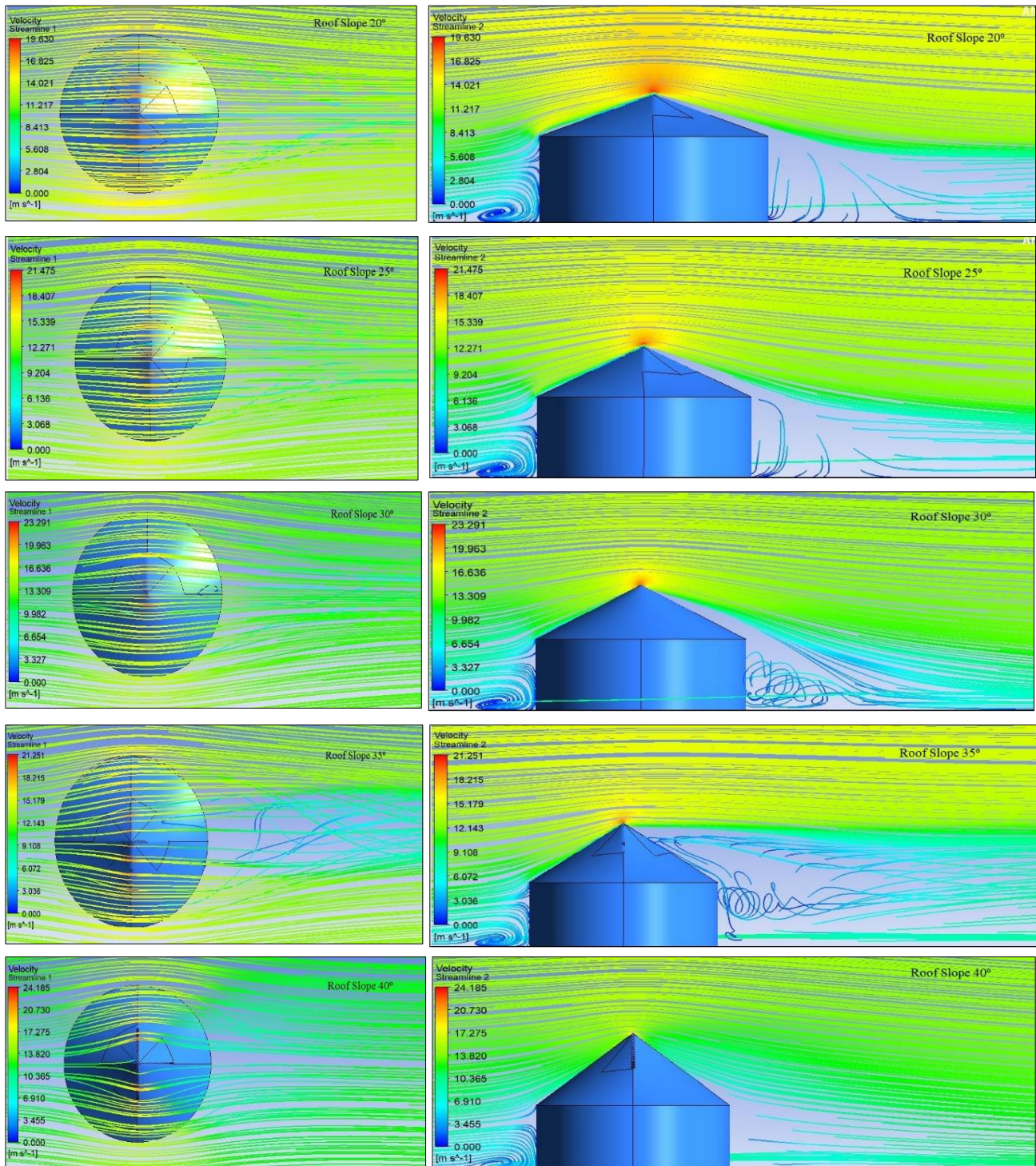


Figure 9: Velocity streamlines around the building model for 0° to 30° roof slopes @10° intervals for 0° wind directions

the case of 20° and 25° roof slope, the pattern of higher pressure coefficients is like a candle flame on both sides of the centerline (along wind direction). In case 35 and 40°, it shows a pattern like a torchlight, and a 30° roof slope shows a pattern like a bulb. All these patterns show the effect of roof slope on wind load distribution.

A variation of maximum positive pressure coefficient, maximum negative pressure coefficient, and area-weighted average pressure coefficient has been shown through the graphical representation in

Figure 8. The maximum positive pressure coefficient is displayed by red color, the blue color represents the maximum negative pressure coefficient, while the area-weighted average pressure coefficient is shown by green color.

The maximum positive pressure coefficients for the roof slope 20° to 30° are almost the same and, also for 35° and 40° roof slope, the pressure coefficients are of small magnitude, which means there is a minimal variation in maximum positive pressure coefficients and are not much significant.

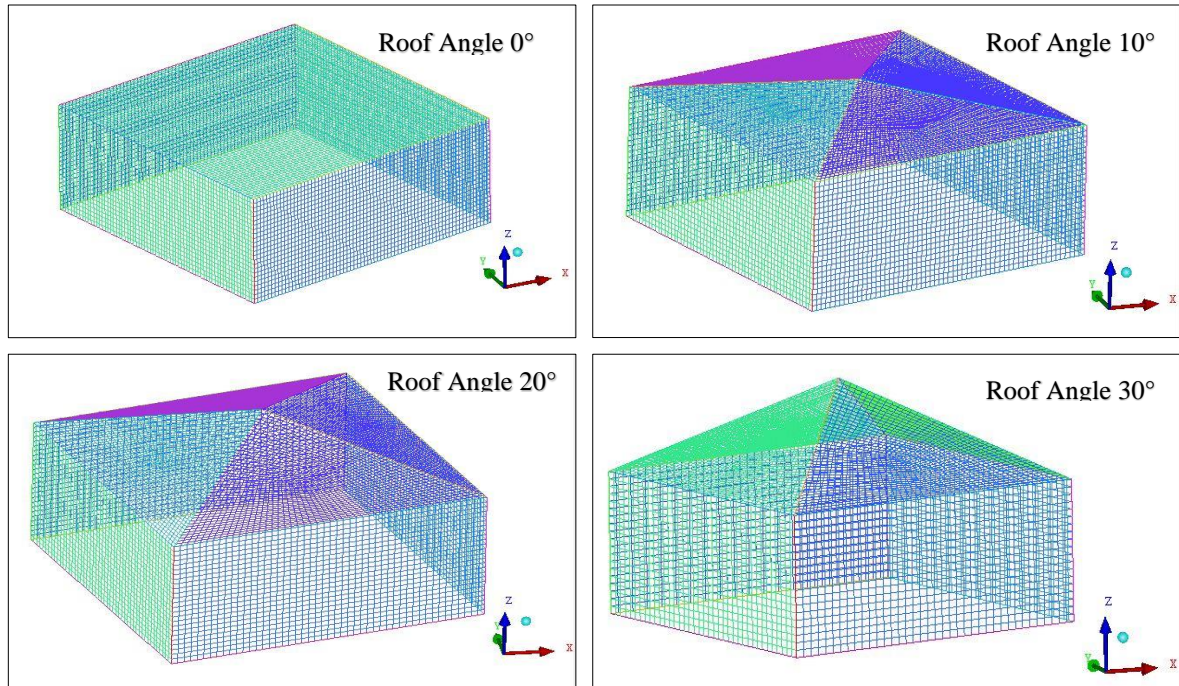


Figure 10: Hexagonal mesh for different square plan pyramidal models

While in the case of maximum negative pressure coefficient, there is a considerable variation in pressure coefficients, which maybe because of the increase in vortices and whirls with a change in roof slope. The area-weighted average pressure coefficient for all the roof slopes has also shown an unnoticeable variation.

The 35° roof slope is found as the optimum roof angle for the present study, as there is the least area-weighted average pressure coefficient for this roof angle. The roof slope 30° is found the most critical roof angle in terms of wind load resistance among all the roof angles of the present study.

### 3.3 Velocity Streamlines

The velocity streamlines for different roof slopes on a horizontal plane and vertical plane has been illustrated in Figure 9. The horizontal plane is taken at the height of 110 mm so that the effect of roof inclination on velocity streamlines can be observed as the eave height in the case of all roof slopes is 95 mm. In contrast, the vertical plane has been taken at the center of the building models along the wind direction. The color variation illustrates the magnitude of the velocity. And the deviation in the streamlined path is represented by the curved lines. The red color represents the highest velocity in all cases, while the dark blue color demonstrates the lowest wind velocity.

The horseshoe vortex can be seen on the upward wind side near the base in all the roof angle cases. The obstruction of flow by the cylindrical wall

results in a stagnation line on the front of the cylindrical wall. As we recall from the fundamentals of fluid dynamics, the stagnation pressure is higher than the hydrostatic pressure by an amount equivalent to the dynamic pressure.

The dynamic pressure is proportional to the square of the local velocity and is lower near the bed. Therefore, a downward hydraulic gradient develops in front of the building model wall that causes downflow directed towards the bed, as shown in Figure 9.

From streamlines on a horizontal plane, it can be observed that there is very little disturbance in wind flow at the height of 110 mm. The streamlines get scattered more on the roof surface with increasing roof slope, and the same may be noticed from the streamlines on a horizontal plane. The highest wind velocity is seen in the case of 40° roof slope. That may be because of roof slope steepness, which causes a decrease in roof surface area that is in direct contact with the wind.

As the velocity streamlines on a vertical plane have been drawn at the center of the building model, similar vortices can be seen on the windward side of the model. While on the leeward side, there is little turbulence near the model in case of a 30° and 35° roof angle. The absence of velocity streamlines near the model on the downwind side is the highest for a 40° roof slope. And this causes the highest negative pressure on the roof surface. The highest wind velocity is observed near the apex of each of the building models because of the roof shape, after

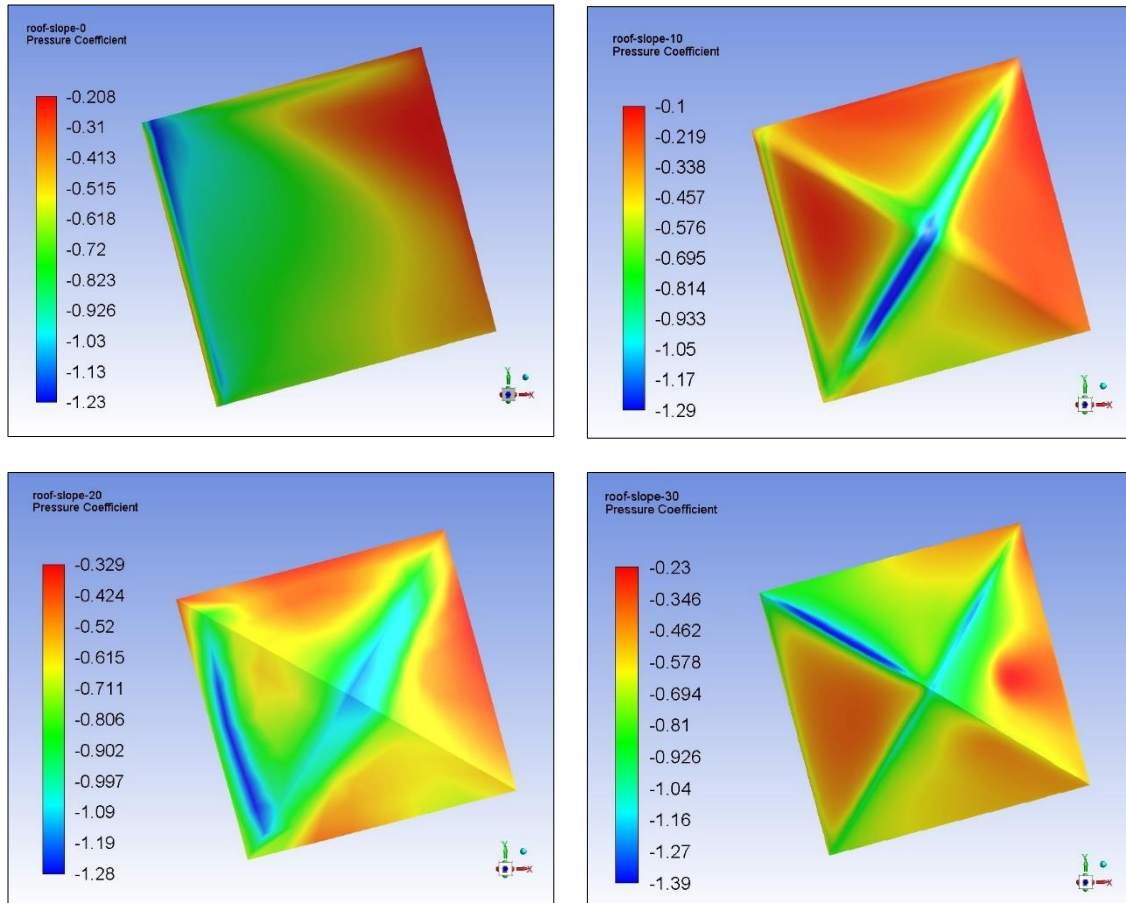


Figure 11: Pressure coefficients on roof surface for 15° wind angle from CFD simulation

striking on the conical surface, the wind gets faster quickly.

#### 4. VALIDATION

For the validation of the study, numerical simulation has been carried out for a pyramidal roof low-rise building and the results are compared with the wind tunnel results from Roy et al study [24]. The square pyramidal roof model (base 225×225 cm) with four roof slopes i.e. 0°, 10°, 20°, and 30° for 15° wind angle has been created in Icem CFD with the same size of the domain. The 3-D building models and the meshing have been carried out in Ansys Icem. The hexagonal grid for all the models have been shown in Figure 10.

The k-epsilon turbulence model has been used for the simulation in Ansys Fluent. The remaining parameters i.e. boundary conditions, velocity profile, turbulence intensity are also taken from the reference study.

In Figure 11, the contours of pressure coefficients for all four models have been illustrated with minimum and maximum values of pressure coefficients on the roof surface. Change in pressure distribution with varying roof slopes can be seen in

all contours. And in Figure 12, a comparison between CFD values for maximum negative pressure coefficient and experimental values is shown. The CFD values were found larger than experimental values by an extent of 35%, 33%, 28%, and 32% for roof slopes 0°, 10°, 20°, and 30° respectively. And this difference between CFD and experimental values seem admissible. So the CFD results are valid.

#### 5. LIMITATIONS OF THE PRESENT STUDY

The two main objectives of the current research work on the conical roofed structure are: (1) To

Comparison between experimental and CFD results

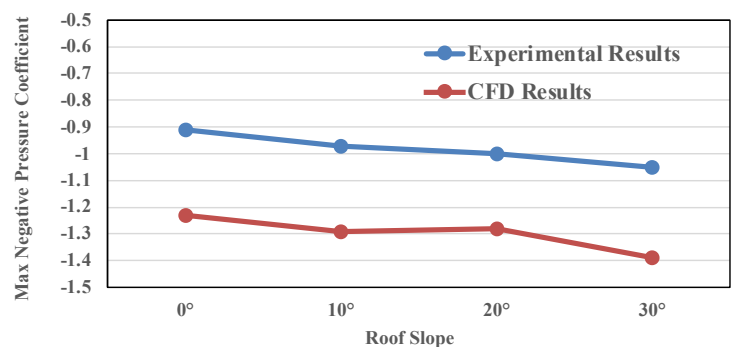


Figure 12: Comparison between experimental and CFD values

estimate the influence of the roof inclination angle on the variation of wind pressure coefficients and (2) To observe the wind flow behavior near the building model. The impact of four roof inclination angles is estimated ( $0^\circ$  to  $40^\circ$ ). It seems essential to indicate the limits of the existing study, upon which investigation may be carried out in the future:

- The current study is all about basic single-story buildings. The influence of other building aspects such as opening, eaves, and inside arrangement may be examined.
- As the simulation of an isolated building is carried out in the present study, the interference effect should be studied for the proper understanding of the pressure deviation on the roof.
- In the existing study, all building models have the same height, and the building has a height to width ratio of  $\frac{h}{w} \leq \frac{1}{2}$  stated in the IS-875(Part-3):2015[29]. Other height to width ratio mentioned in IS-875 can also be investigated.

By displaying and analyzing the velocity streamlines, and all the pressure coefficient contours, the influence of the roof slope has been investigated. Further, the research work may be explored up to some extent by the investigation of the building models for some other larger roof slopes and some other forms of openings.

## 6. CONCLUSIONS

The current study describes the impact of the roof slope on the distribution of wind pressure over the surface of the conical roofed low-rise building. The simulation has been carried out in ANSYS Fluent to produce the results which have been displayed in the form of contours and graphs of pressure coefficients and velocity streamlines. The foremost conclusion points derived from the study are specified below:

- The present study indicates that the realizable  $k-\epsilon$  turbulence model offers almost the precise outcomes. And it can simulate the horizontal homogeneity of velocity profiles.
- The horizontal homogeneity is the comparison among different velocity profiles and the deviation of velocities at the upwind side of the building model in the computational domain. It is noticed that at building model height, the wind speed is near about 11 m/s, validating the velocity profile.

- Among all the wind angles, the highest maximum positive wind pressure coefficient is found as 0.24 in case of a  $40^\circ$  roof angle, while the highest maximum negative pressure coefficient (suction) is seen as -2.1 in the case of  $30^\circ$  roof slope.
- It is observed from the pressure coefficient contours that the area of negative pressure increases with the increasing roof slope as the higher roof slopes cause more vortices and whirls around the model. Also, the variation of pressure coefficients shows a symmetrical pattern for all the roof slopes along the centerline (along wind direction).
- The  $35^\circ$  roof slope is found as the optimum roof angle for the present study as there is the least area-weighted average pressure coefficient for this roof angle. The roof slope  $30^\circ$  is found the most critical roof angle in terms of wind load resistance among all the roof angles of the present study.
- The streamlines on the vertical plane show horseshoe vortex in the case of all roof slopes, and it is due to the pressure gradient on the windward side near the bottom of the model.
- From streamlines on a horizontal plane, it can be observed that there is very little disturbance in wind flow at the height of 110 mm. The streamlines get scattered more on the roof surface with increasing roof slope, and the same may be noticed from the streamlines on a vertical plane.

## ACKNOWLEDGMENT

I would like to convey my exceptional thanks and appreciation to my Institution NIT Hamirpur, H.P., for providing resources and to the Ministry of Human Resource Development, India for providing research assistantship. I also thank my friends Kanika Sharma and Sakshi Goyal for helping me in this project. This research was funded by "Ministry of Human Resource Development, INDIA" as a PhD Assistantship.

## REFERENCES

- [1] N. Lott and T. Ross, (2005), Tracking and Evaluating U.S. Billion Dollar Weather Disasters, 1980-2005., 2005.
- [2] S. A. Hsu, (2008), Estimating 3-second and maximum instantaneous gusts from 1-minute sustained wind speeds during a hurricane., Electron. J. Struct. Eng., 200877-79.

- [3] P. Mendis, T. Ngo, N. Haritos, and A. Hira, (2007), Wind Loading on Tall Buildings., *Electron. J. Struct. Eng.*, 200741–54no. Special Issue: Loading on Structures.
- [4] R. Calculator, (2019), Top 20 Roof Types and Pros & Cons – Roof Styles, Design & Architecture., [www.roofingcalc.com](http://www.roofingcalc.com), 2019. [Online]. Available: <https://www.roofingcalc.com/top-20-roof-types/>. [Accessed: 23-Aug-2019].
- [5] S. K. Verma, A. K. Roy, S. Lather, and M. Sood, (2015), CFD Simulation for Wind Load on Octagonal Tall Buildings., *Int. J. Eng. Trends Technol.*, 2015211–216vol. 24, no. 4.
- [6] H. Sadeghi, M. Heristchian, A. Aziminejad, and H. Nooshin, (2018), CFD simulation of hemispherical domes: structural flexibility and interference factors., *Asian J. Civ. Eng.*, 2018vol. 5.
- [7] R. Ahuja, S. K. Dalui, and V. K. Gupta, (2006), Unpleasant pedestrian wind condition around buildings., *Asian J. Civ. Eng.*, 2006147–154vol. 7, no. 2.
- [8] M. Yahyai and M. Z. and S. M. M. , Amir Saedi Daryan, (2011), Wind effect on milad tower using computational fluid dynamics., *Struct. Des. Tall Spec. Build.*, 2011177–189vol. 20, no. 2.
- [9] M. R. Heidari, M. R. Soltani, and M. Farahani, (2010), Computational and Experimental Investigations of Boundary Layer Tripping., *J. Appl. Fluid Mech.*, 201053–63vol. 3, no. 2.
- [10] N. Belkheir, R. Dizene, and S. Khelladi, (2012), A Numerical Simulation of Turbulence Flow around a Blade Profile of HAWT Rotor in Moving Pulse., *J. Appl. Fluid Mech.*, 20121–9vol. 5, no. 1.
- [11] M. Llaguno-Munitxa, E. Bou-Zeid, and M. Hultmark, (2017), The influence of building geometry on street canyon air flow: Validation of large eddy simulations against wind tunnel experiments., *J. Wind Eng. Ind. Aerodyn.*, 2017115–130vol. 165, no. March.
- [12] P. S. Kumar, A. Abraham, R. J. Bensingh, and S. Ilangovan, (2013), Computational and Experimental analysis of a Counter-Rotating Wind Turbine system., *J. Sci. Ind. Res. (India)*, 2013300–306vol. 72, no. May.
- [13] B. Bhattacharyya, S. K. Dalui, and A. K. Ahuja, (2014), Wind Induced Pressure on “ E ” Plan Shaped Tall Buildings., *Jordan J. Civ. Eng.*, 2014120–134vol. 8, no. 2.
- [14] Q. Zhou and L. D. Zhu, (2020), Numerical and experimental study on wind environment at near tower region of a bridge deck., *Heliyon*, 2020e03902vol. 6, no. March.
- [15] ASCE Standard, (2016), Wind Loads (ASCE/SEI 7-16).245–390.
- [16] E. Standard, (2010), Eurocode 1: Actions on structures - Part 1-4: General actions - Wind actions.
- [17] N. Z. S. and A. Standard, (2011), Structural design actions - Part 2: Wind actions (AS/NZS 1170.2:2011), vol. 2. vol. 2.
- [18] B. of I. Standards, (2015), Design loads (other than earthquake) for buildings and structures - code of practice Part 3 Wind Loads, IS 875-3. .
- [19] B. S. Institution, (1997), BS 6399-2: 1997 British Standard, Loading for buildings-Part 2: Code of practice for wind loads, vol. 2. vol. 2.
- [20] ASCE/SEI 7-16, (2017), Minimum design loads and associated criteria for Buildings and Other Structures. .
- [21] J. Singh and A. Kumar, (2019), CFD simulation of the wind field around pyramidal roofed single - story buildings., *SN Appl. Sci.*, 2019vol. 1, no. 1425.
- [22] D. K. and R. S. Shreyas Ashok Keote, (2015), Construction of Low Rise Buildings in Cyclone Prone Areas and Modification of Cyclone Construction of Low Rise Buildings in Cyclone Prone Areas and Modification of Cyclone., *J. Energy Power Sources*, 2015247–252vol. 2, no. July.
- [23] A. K. Roy, J. Singh, S. K. Sharma, and S.K. Verma, (2018), Wind pressure variation on pyramidal roof of rectangular and pentagonal plan low rise building through CFD simulation., *Int. Conf. Adv. Constr. Mater. Struct.*, 20181–10.
- [24] A. K. Roy, N. Babu, and P. K. Bhargava, (2012), Atmospheric Boundary Layer Airflow Through Cfd Simulation on Pyramidal Roof of Square Plan Shape Buildings., no. December 2012291–299no. December 2012.
- [25] J. Revuz, D. M. Hargreaves, and J. S. Owen, (2012), On the domain size for the steady-state CFD modelling of a tall building., *Wind Struct. An Int. J.*, 2012313–329vol. 15, no. 4.
- [26] Ansys, (2007), Ansys ICEM CFD 11 . 0 Tutorial Manual. .
- [27] A. K. R. and A. G. A. D. John, (2012), Wind Loads on Walls of Low-Rise Building., no. December449–456no. December.
- [28] M. N. M. L. E. Jabbari, (2016), Numerical Simulation of Turbulent Flows Using a Least Squares Based Meshless Method., *Int. J. Civ. Eng.*, 201677–87vol. 15.
- [29] 2015 IS: 875 (part-3), (2015), IS 875-3 Design loads (other than earthquake) for buildings and structures - code of practice .pdf. 2015, 2015.